

Reduction of Co-Channel Interference in GSM by Joint Channel and Data Estimation

Maja Lončar, Christoph F. Mecklenbräuker, Ralf R. Müller

Telecommunications Research Center Vienna (ftw.)
Tech Gate Vienna, Donau-City Str. 1/III, A-1220 Vienna, Austria

Ph.: +43 1 505 2830 40, Fax: +43 1 505 2830 99, E-mail: loncar@ftw.at

ABSTRACT

Multiuser detection is a powerful tool for combating co-channel interference in multiple-access communication systems [1]. In this paper, we investigate the feasibility of achieving increased spectral efficiency in GSM-like TDMA networks by applying multiuser detection. Two special cases are considered: In the first scenario, two users are served simultaneously in the same cell. In the second one, two users in adjacent cells are served on the same frequency. We focus on downlink operation. Multiple receive antennas at the mobile terminals provide the processing gain necessary to enable efficient multiuser detection. We propose an efficient iterative receiver structure that performs joint channel estimation and data detection. The performance is evaluated by means of simulations.

1. INTRODUCTION

Existing cellular networks are faced with an ever increasing demand for higher throughput, in terms of the number of users that can be simultaneously served. In a GSM network, the number of users in a cell is system-limited: every cell is assigned a set of frequency bands, each of them can accommodate 8 users in different time slots. Adjacent cells use different sets of bands in order to minimize inter-cell interference. Strict power control within each cell further reduces interference level [2].

A physical communication channel in a single cell is uniquely defined for each user with a time slot number and a pair of uplink and downlink carriers. Physical content of a time slot is called *burst*, with a structure as shown in Fig. 1. A midamble defined by the Training Sequence Code (TSC), placed in the center of each burst, is used for estimation of radio channel conditions. Hereinafter, guard period (GP) and tail binary symbols (TB) will be ignored, and only $N_{burst} = 142$ useful binary symbols will be referred to as a user's burst.

In this paper, we investigate the case when two users share the same physical channel. If a properly designed receiver can combat strong co-channel interference that would arise in such a case, it would allow significant improvement of the network throughput.

Two scenarios should be distinguished:

- interfering users belong to the same cell (*intra-cell interference*)
- interfering users belong to adjacent cells (*inter-cell interference*)

Our further attention will be mainly focused on the latter case. We will consider downlink communication from the base station to a multiple antenna mobile receiver. Signal and channel model are given in Section 2. Channel estimation is addressed in Section 3. The receiver structure is proposed in Section 4. Section 5 analyzes the receiver's performance. Finally, Section 6 summarizes our work.

2. SIGNAL AND CHANNEL MODEL

While propagating through the radio channel, the signal is subject to different time-varying distortions due to interference, fading and noise. For our investigation, we will consider a simplified case of a flat fading channel that does not induce inter-symbol interference. In this case, apart from additive noise, the channel introduces only an unknown attenuation that scales the signal amplitude. The total attenuation is the result of several processes that are assumed to be mutually independent [3]:

1. *Path loss*: Signal power decreases according to the power law of the distance between the transmitter and the receiver. In the general case, the path loss attenuation can be expressed as [4]:

$$\frac{|a|^2}{a_0^2} = \left(\frac{r}{r_0}\right)^{-\alpha},$$

where α is the path loss exponent that depends on the environment, a and a_0 are amplitude weights at distance r and reference distance r_0 , respectively.

2. *Large scale fading (shadowing)* is due to large obstacles in the propagation path that block the signal. It is a slowly varying process, modelled stochastically with log-normal distribution:

$$20 \log(s) [\text{dB}] \sim \mathcal{N}(\mu_s, \sigma_s^2)$$

3. *Small scale fading* is the result of multipath propagation. The amplitude of the received faded signal is modelled as a random variable with Rayleigh distribution.

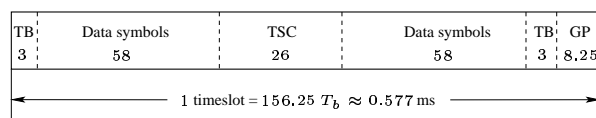


Figure 1: Normal burst in GSM

Two scenarios are of interest:

- Let us first consider two co-channel users served by the same base transceiver station (BTS). The cell is modelled as a circular area of radius R , with the BTS in the center and the users uniformly, independently identically distributed (i.i.d.) inside. Let us denote the mobile user of interest as MS_1 and the interfering user as MS_2 , with all the associated parameters indexed correspondingly. If we assume perfect power control performed in the downlink, the path loss and shadowing attenuation of MS_1 's signal will be compensated for. However, the interfering signal will be received at MS_1 attenuated by relative shadowing and path loss coefficients given respectively by:

$$s = \frac{s_1}{s_2} ; \quad p = \frac{p_1}{p_2} = \left(\frac{r_1}{r_2} \right)^{-\alpha/2} .$$

The baseband signal model can be expressed as:

$$\mathbf{y}(i) = x_1(i) \mathbf{h}_1 + s p x_2(i) \mathbf{h}_2 + \mathbf{n} \quad (1)$$

where $\mathbf{y}(i)$ is $(1 \times N_a)$ vector of the received signals at N_a antennas of MS_1 at i -th symbol interval, $i = 1, 2, \dots, N_{burst}$; $x_1, x_2 \in \{-1, +1\}$ are i -th transmitted symbols from BTS to MS_1 and MS_2 , \mathbf{n} is a complex Gaussian noise vector (zero mean, with variance σ^2) and \mathbf{h}_1 and \mathbf{h}_2 are channel impulse response vectors containing i.i.d. complex Gaussian coefficients for each receiving antenna. Thus, they can be viewed as unique spatial signatures characterizing each user's signal space almost surely. This is analogous to spreading with signature sequences in CDMA systems [5].

- The scenario when two interfering users belong to two adjacent cells is illustrated in Figure 2. In this case, the same signal model given with (1) holds, except that the relative attenuation weights are given by:

$$s = \frac{s_{21}}{s_2} ; \quad p = \frac{p_{21}}{p_2} = \left(\frac{r_{21}}{r_2} \right)^{-\alpha/2} , \quad (2)$$

with the notation corresponding to Figure 2. Due to larger distance range between MS_1 and the interfering base station BS_2 , $r_{21} \in [R, 3R]$, interference can undergo much larger path loss attenuation than in previous case.

Path loss and shadowing are slowly varying processes that do not change significantly over several time slots. That enables reliable estimation of coefficients s and p , which are therefore assumed to be perfectly known to the receiver in our model. However, Rayleigh fading coefficients may change rapidly from one slot to another and therefore need to be estimated for each burst. They are considered to be invariant during one burst duration.

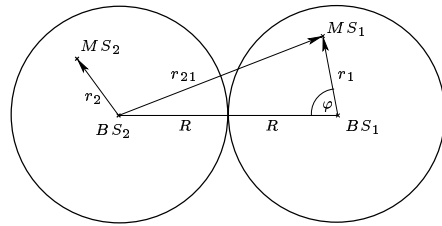


Figure 2: Two users in adjacent cells

3. CHANNEL ESTIMATION

3.1. Users in the Same Cell

Since both the useful and the interfering signal arrive to the mobile receiver from the same BTS, bursts will be completely overlapped, as shown in Fig. 3. Due to attenuation, powers differ significantly, in general. The midamble parts \mathbf{d}_1 and \mathbf{d}_2 will be perfectly aligned. Therefore, in order to enable identification and estimation of different channels for each user, it is necessary that they use different midambles. We assume that MS_1 knows the interferer's midamble \mathbf{d}_2 .

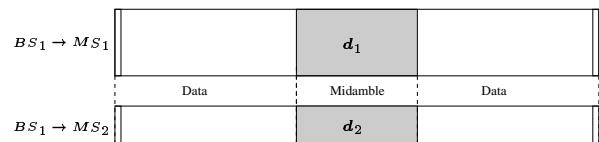


Figure 3: Overlapping bursts

If we stack $N_d = 26$ vectors given by (1) into $(N_d \times N_a)$ matrix of midamble part of the received signal, we can write

$$\mathbf{Y}_d = \mathbf{d}_1 \mathbf{h}_1 + s p \mathbf{d}_2 \mathbf{h}_2 + \mathbf{N}, \quad (3)$$

where $\mathbf{d}_i = (m_0^{(i)} m_1^{(i)} \dots m_{25}^{(i)})^T$, $i = 1, 2$ denote¹ the midamble sequences. This can be written in matrix form:

$$\mathbf{Y}_d = \mathbf{D} \mathbf{H} + \mathbf{N}$$

$$\mathbf{D}_{26 \times 2} = [\mathbf{d}_1 \quad s p \mathbf{d}_2] ; \quad \mathbf{H}_{2 \times N_a} = [\mathbf{h}_1^T \quad \mathbf{h}_2^T]^T. \quad (4)$$

The linear least squares (LS) estimator [6] gives the estimated channel matrix:

$$\hat{\mathbf{H}} = \mathbf{D}^\# \mathbf{Y}_d = (\mathbf{D}^T \mathbf{D})^{-1} \mathbf{D}^T \mathbf{Y}_d. \quad (5)$$

Joint channel estimation for both users takes into account non-zero cross-correlation between the midambles. In case the midambles are orthogonal, i.e. $\mathbf{d}_i^T \mathbf{d}_j = 0$, channel estimates of both users will not be influenced by the each other user's channel, but by noise only.

3.2. Users in Adjacent Cells

The interfering signal now arrives from the base station in the neighbouring cell. A significant difference compared to the previous case is lack of synchronization between different base stations. Thus, a random offset between signals will occur. It can have arbitrary value from

¹ $(\cdot)^T, (\cdot)^H$ denote matrix transposition and Hermitian transpose, respectively.

0 to burst duration, but, for the sake of simplicity, it is assumed here that it can take only integer values of symbol duration T_s . Then, normalized offset values are in the range of:

$$N_{offset} = \frac{T_{offset}}{T_s} = 0, 1 \dots 141.$$

The value of the offset is considered to be known at the receiver side. Figure 4 depicts the case for $59 \leq N_{offset} \leq 84$, when the midamble part of the second signal is "split" into two parts.

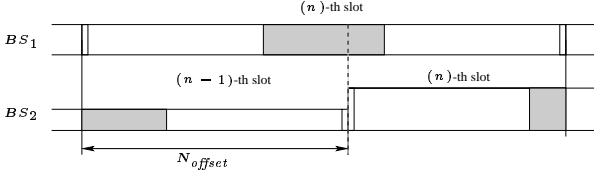


Figure 4: Offset bursts

One burst will be affected by two unequal power interferers from two adjacent time slots. They are transmitted with different powers, but they share the same channel, since they arrive from the same base station. Then, the received burst on all the antennas can be written as

$$\mathbf{Y} = \mathbf{x}_1 \mathbf{h}_1 + \tilde{\mathbf{x}}_2 \mathbf{h}_2 + \mathbf{N}, \quad (6)$$

where

$$\mathbf{x}_1 = [x_1(1) \ x_1(2) \ \dots \ x_1(N_{burst})]^T$$

$$\tilde{\mathbf{x}}_2 = [s'p'x_2(1, \dots, N_{offset}) \ s''p''x_2(N_{offset}+1, \dots, N_{burst})]^T.$$

Obviously, midambles are not aligned any more, but overlap with unknown data bits. Therefore, channel estimation should be done jointly with data detection [7]. A simple iterative method is explained in the next section.

4. RECEIVER STRUCTURE

A block diagram of the iterative receiver is shown in Fig. 5. Initial channel estimates are obtained separately, regarding the other signal as noise:

$$\hat{\mathbf{h}}_1^{(0)} = \frac{1}{26} \mathbf{d}_1^T \mathbf{Y}_{d_1}; \quad \hat{\mathbf{h}}_2^{(0)} = \frac{1}{26} \mathbf{d}_2^T \mathbf{Y}_{d_2}, \quad (7)$$

where \mathbf{Y}_{d_1} and \mathbf{Y}_{d_2} contain the midamble of user 1 and user 2, respectively. Comparing estimates in (7) and taking into account known attenuation of the interference, it is determined which signal is stronger. Iterations start with detection of that signal, setting the weaker channel estimate back to zero. Without loss of generality, let us assume signal from BS_1 is stronger, and therefore we set $\hat{\mathbf{h}}_2^{(0)} = 0$. In each iteration step $j = 1, \dots, M$, channel estimates are improved using the previously obtained estimates of the data bits that overlap with midambles:

$$\begin{aligned} \hat{\mathbf{h}}_1^{(j)} &= \frac{1}{26} \mathbf{d}_1^T \left(\mathbf{Y}_{d_1} - \tilde{\mathbf{x}}_{2d_1}^{(j-1)} \hat{\mathbf{h}}_2^{(j-1)} \right) \\ \hat{\mathbf{h}}_2^{(j)} &= \frac{1}{26} \mathbf{d}_2^T \left(\mathbf{Y}_{d_2} - \tilde{\mathbf{x}}_{1d_2}^{(j)} \hat{\mathbf{h}}_1^{(j)} \right). \end{aligned} \quad (8)$$

For intermediate decisions used as feedback information in the iterative process, a soft decision rule is applied. For

the binary signals in Gaussian noise, it can be shown that the optimal soft decision function in terms of minimizing mean square estimation error (MSE) is the hyperbolic tangent, with the slope determined by signal-to-noise ratio (SNR), cf. Fig. 6. Thus, tentative decisions in the i -th iteration are given by ([8], [9]):

$$\tilde{\mathbf{x}}_1^{(j)} = \tanh \left\{ S\hat{N}R^{(j)} \cdot \text{Re} \left[\hat{\mathbf{h}}_1^{H(j)} \left(\mathbf{Y} - \tilde{\mathbf{x}}_2^{(j-1)} \hat{\mathbf{h}}_2^{(j-1)} \right) \right] \right\}$$

$$\tilde{\mathbf{x}}_2^{(j)} = \tanh \left\{ S\hat{N}R^{(j)} \cdot \text{Re} \left[\hat{\mathbf{h}}_2^{H(j)} \left(\mathbf{Y} - \tilde{\mathbf{x}}_1^{(j)} \hat{\mathbf{h}}_1^{(j)} \right) \right] \right\}.$$

The estimates of SNR are updated in each iteration as

$$S\hat{N}R^{(j)} = \frac{\|\hat{\mathbf{h}}_1^{(j)}\|^2}{\hat{\sigma}^2} \quad (9)$$

$$\hat{\sigma}^2 = \frac{1}{N_a} \text{trace} \{ \hat{\mathbf{P}}_{\mathcal{H}}^\perp \hat{\mathbf{C}}_y \}, \quad (10)$$

where the $(N_a \times N_a)$ signal covariance matrix and the projection matrix associated with the noise space are defined by

$$\hat{\mathbf{C}}_y = \text{E} \{ (\mathbf{y}^T)(\mathbf{y}^T)^H \} = \mathbf{H}\mathbf{H}^H + \sigma^2 \mathbf{I} \quad (11)$$

$$\hat{\mathbf{P}}_{\mathcal{H}}^\perp = \mathbf{I} - \mathbf{H}(\mathbf{H}^H \mathbf{H})^{-1} \mathbf{H}^H \quad (12)$$

taking into account that in (1) \mathbf{y} , \mathbf{h}_1 , and \mathbf{h}_2 were defined as row vectors. The estimated matrices are obtained in the following way:

$$\hat{\mathbf{C}}_y = \frac{1}{N_{burst}} \sum_{i=1}^{N_{burst}} (\mathbf{y}_i^T)(\mathbf{y}_i^T)^H \quad (13)$$

$$\hat{\mathbf{P}}_{\mathcal{H}}^\perp = \mathbf{I} - \hat{\mathbf{P}}_{\mathcal{H}} = \mathbf{I} - \mathbf{Q}^H \mathbf{Q}, \quad (14)$$

where $\mathbf{Q} = \text{orth}(\hat{\mathbf{H}})$ spans the same estimated signal subspace $\hat{\mathcal{H}}$ as $\hat{\mathbf{H}}$, but has orthogonal columns.

The iterative process converges rapidly. Simulations show that after $M = 3$ iterations channel estimates reach steady state, thus allowing to stop the iterations with final data symbol estimates. They are obtained by applying the hard decision rule

$$\hat{\mathbf{x}}_1 = \text{sign} \left\{ \text{Re} \left[\hat{\mathbf{h}}_1^{H(M)} \left(\mathbf{Y} - \tilde{\mathbf{x}}_2^{(M)} \hat{\mathbf{h}}_2^{(M)} \right) \right] \right\}$$

$$\hat{\mathbf{x}}_2 = \text{sign} \left\{ \text{Re} \left[\hat{\mathbf{h}}_2^{H(M)} \left(\mathbf{Y} - \tilde{\mathbf{x}}_1^{(M)} \hat{\mathbf{h}}_1^{(M)} \right) \right] \right\}.$$

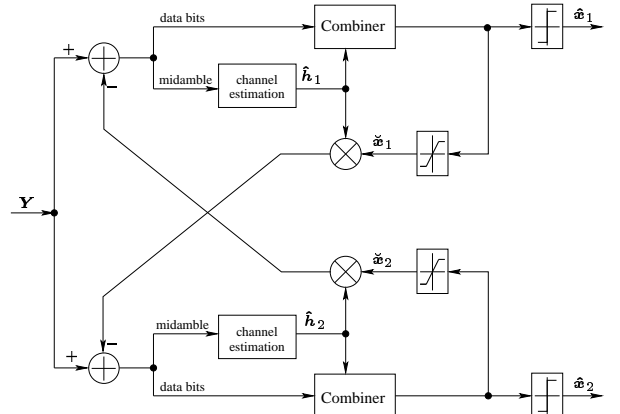


Figure 5: Block diagram of iterative receiver

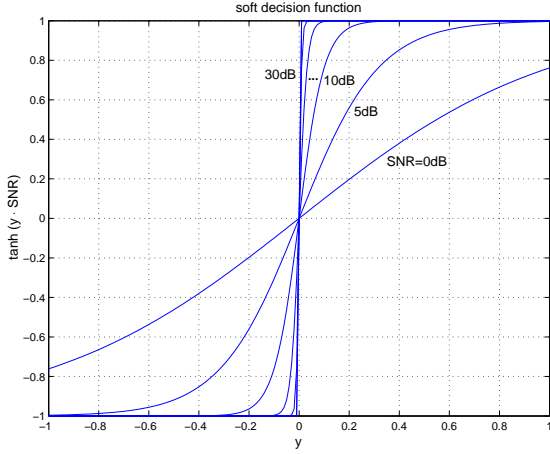


Figure 6: Soft decision function for binary symbols

5. BIT ERROR RATE PERFORMANCE

As a performance measure of the receiver, we observe the bit error rate for different levels of mean signal-to-noise ratio (SNR), which is defined as

$$SNR = \frac{\overline{E_s}}{N_0},$$

where $\overline{E_s}$ is mean energy per symbol and N_0 is one-sided power density spectrum of white noise.

The results for the scenario with users in adjacent cells are discussed first. Attenuation weights are defined via (2), where path loss exponent is $\alpha = 4$ and standard deviation of shadowing is the same for both cells $\sigma_{21} = \sigma_2 = 10$ dB. These values, which are standard for modelling urban and suburban environment [10], lead to huge variations of interference power. Averaged over all possible path loss values (for all possible relative positions of the mobile users) signal to interference (SIR) level amounts to -6 dB. In the performed simulations it was assumed that the positions of the users change from one burst to another, thus leading to independent, different instantaneous interference levels for both the interferers. Figure 7 shows results obtained for variable number of iterations in the receiver that exploits $N_a = 4$ antennas.

The BER of the receiver is compared to the analytical result for probability of error for binary symbols in a Rayleigh fading channel, with L statistically independent diversity branches. A closed-form solution for such a case is given by [11]:

$$P_\epsilon = \left(\frac{1}{2}(1-\mu)\right)^L \sum_{k=0}^{L-1} \left[\binom{L-1+k}{k} \left(\frac{1}{2}(1+\mu)\right)^k \right], \quad (15)$$

where L in our case equals to the number of antennas N_a , and μ is the function of the average SNR per channel, defined as:

$$\mu = \sqrt{\frac{SNR/N_a}{1 + SNR/N_a}}.$$

Note that expression (15) assumes the perfect knowledge of the channel at the receiver side and completely orthogonal users' signatures. The receiver approaches this

bound after $M = 3$ iterations. A performance gap of less than 1 dB is due to non-ideal channel estimation and highly variable power of shadowed interference.

The performance is highly dependent on the relative offset between the signals arriving from the serving and the interfering base station. Due to symmetry, relative offset is defined as: $N_{rel} = (N_{offset} - \frac{1}{2}N_{burst}) \in \{-71, \dots, 0, \dots, 70\}$. The results shown in Fig. 7 are obtained for $N_{rel} = 2$. In case of perfect synchronism ($N_{rel} = 0$), the BER closely follows the bound (15) for all SNRs. However, for higher values of temporal offsets, the performance decreases significantly and the BER curve flattens out at high SNR.

The influence of relative offset on BER is also depicted by Fig. 8, which shows the behaviour of the BER for two levels of SNR. For higher SNR (lower curve), interference is dominant over noise, therefore the receiver will be much more sensitive to channel estimation errors. Both curves show that for small relative offsets, when almost the whole burst is affected by the same level of interference, the receiver is able to mitigate this interference throughout iterations.

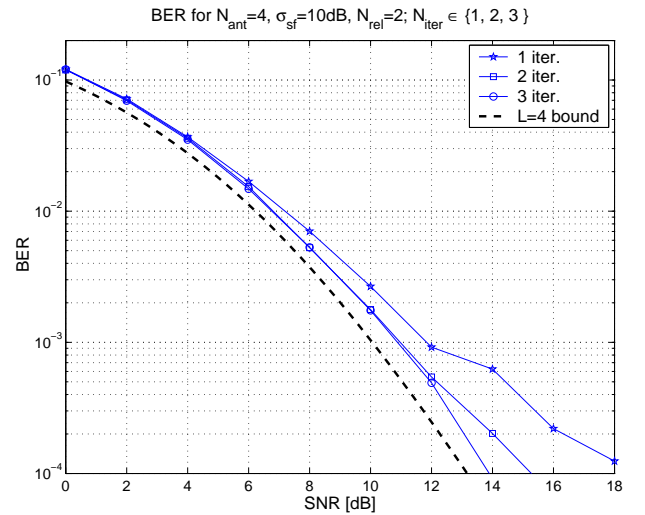


Figure 7: Influence of number of iterations

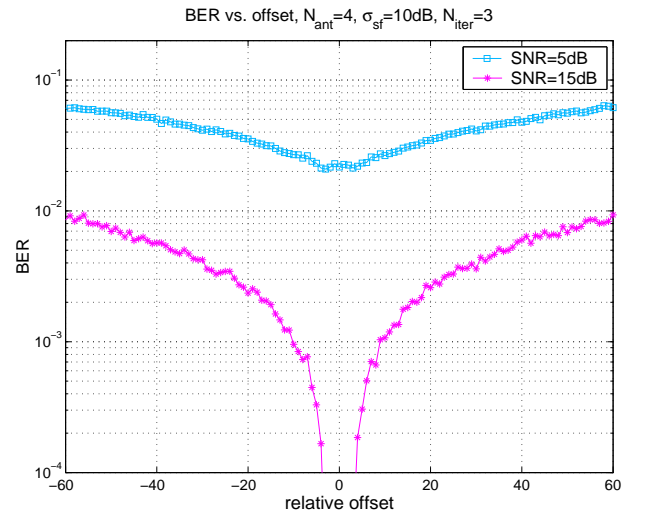


Figure 8: BER for different relative offset

In the light of shown results, it is reasonable to require only a coarse synchronization between the two base stations. It is enough to achieve a relative offset that is not larger than 5 bit durations. Recall that our receiver assumes arbitrary offset and thus considers the bits that interfere with training sequence initially unknown. Under the constraint of $|N_{rel}| \leq 5$, the receiver can be further improved by exploiting the knowledge of the $N_d - |N_{rel}|$ overlapping bits of known training sequences. Initial channel estimates can be obtained by applying the least squares method (5) on the overlapping parts of midambles. They are further improved throughout the iterative process, which leads to a smaller bit error rate.

Finally, the performance for users in the same cell is assessed. The BER is shown in Fig. 9. Note that the users are synchronized to the same BTS, i.e. $N_{rel} = 0$. In this case, we have assumed perfectly orthogonal TSCs. Not all the pairs of TSCs defined in [2] have this property, but four such pairs do exist. Due to orthogonality of the midambles, the channel estimates do not improve with the number of iterations. The performance is very similar to the case of users in adjacent cells when the temporal offset is small, cf. Fig. 7.

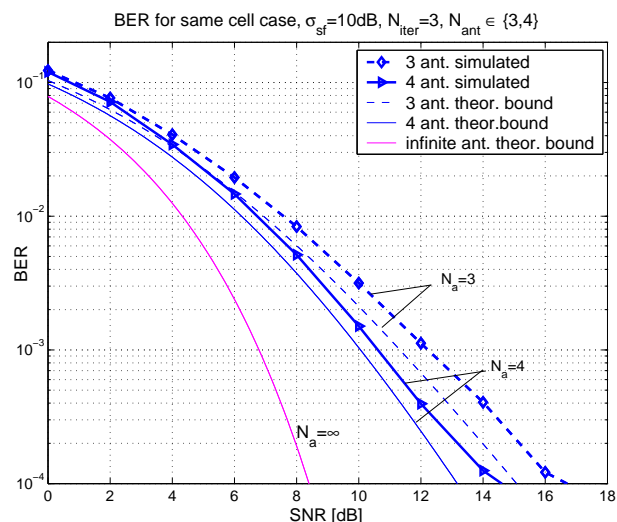


Figure 9: BER in the same-cell scenario

6. SUMMARY AND CONCLUSIONS

In this paper, we propose application of multiuser detection on two asynchronous, power imbalanced co-channel users in a GSM-like system. For a general case of an arbitrary relative offset a low-complexity iterative receiver structure is proposed. It performs joint channel estimation and data detection. Soft decisions on data bits are used as feedback information for updating channel estimates in the iterative process. Simulations indicate that the iterations converge rapidly. Due to large differences between interference levels, receiver's performance strongly depends on the relative offset. It is shown that for small values of relative offsets the BER is close to the lower bound of single-user case in Rayleigh-fading channel. Moreover, the simplified receiver can be extended to handle more than one interfering user.

7. ACKNOWLEDGMENTS

The authors would like to thank Per Ödling (Lund Institute of Technology, Sweden) and Thomas Magesacher (ftw.) for their valuable comments and continuous encouragement and support.

8. REFERENCES

- [1] S. Verdú, *Multuser Detection*, New York, 1998.
- [2] "Digital cellular telecommunications system (phase 2+); multiplexing and multiple access on the radio path, GSM 05.02 version 8.5.0 release 1999," European Standard (Telecommunications Series), Draft ETSI EN 300 908 V8.5.0, July 2000.
- [3] W.C.Y. Lee, *Mobile Communications Engineering*, McGraw-Hill, New York, 1982.
- [4] T.S. Rappaport (Ed.), *Cellular Radio & Personal Communications*, vol. 2: Advanced Selected Readings, IEEE, Piscataway (NJ), 1996.
- [5] S.V. Hanly and D.N.C. Tse, "Resource pooling and effective bandwidths in CDMA networks with multiuser receivers and spatial diversity," *IEEE Trans. Inf. Theor.*, vol. 47, no. 4, pp. 1328–1351, May 2001.
- [6] S. Kay, *Fundamentals of Statistical Signal Processing*, Prentice-Hall, Upper Saddle River, New Jersey, 1993.
- [7] G. Caire, A. Tulino, and E. Biglieri, "Iterative multiuser joint detection and parameter estimation: A factor-graph approach," in *IEEE Proc. Information Theory Workshop*, Cairns, Australia, Sept. 2001.
- [8] R.R. Müller and J.B. Huber, "Iterated soft decision interference cancellation for CDMA," in *Broadband Wireless Communications*, Luise and Papolin, Eds., pp. 110–115. Springer, London, UK, 1998.
- [9] Sgraja C., Teich W., Engelhart A., and Lindner J., "Multiuser/multisubchannel detection based on recurrent neural network structures for linear modulation schemes with general complex-valued symbol alphabet," in *Proceedings of COST 262 Workshop on Multiuser Detection in Spread Spectrum Communications*, Schloss Reisenburg, Ulm, Germany, Jan. 2001, pp. 45–52.
- [10] Members of SMG2, "Selection procedures for the choice of radio transmission technologies of the universal mobile telecommunications system UMTS (UMTS 30.03)," Tech. Rep. ETSI TR 101 112 version 3.2.0, ETSI SMG2, Apr. 1998.
- [11] J. Proakis, *Digital Communications*, McGraw-Hill, New York, 2000.